2021

Investigation of Pressure Drop in Refrigerant Pipes of an Automotive Air Conditioning System

Robin Meinert
Hamburg University of Technology, Hamburg, Germany, robin.meinert@tuhh.de

Gerhard Schmitz

Investigation of Pressure Drop in Refrigerant Pipes of an Automotive Air Conditioning System

Robin MEINERT*, Gerhard SCHMITZ

Hamburg University of Technology, Institute of Engineering Thermodynamics,
Hamburg, Germany
Phone +49 (0)40-42878-2246, Fax +49 (0)40-42878-2967, robin.meinert@tuhh.de

* Corresponding Author

ABSTRACT

This paper presents an experimental and numerical investigation of the pressure drop of automotive refrigerant pipes. The measurement is done with a test rig that is able to set a defined one- or two-phase state at the inlet of an exchangeable test section. With the experimental data, CFD simulations are validated. There is a liquid and a hot gas line being investigated in this work. It turns out that transition pieces between pipe and hose elements have a significant influence on the pressure drop. Although the connection technology is the same, it must always be checked how the internal structure of this transition piece is designed and whether this has an influence on the pressure drop. It is also found that the compressibility of the gas, especially at low pressures and high mass flows, is a physical effect that cannot be neglected and must be implemented in the CFD simulation. All in all, CFD simulations are capable of reproducing the experimental data well after taking these findings into account.

1. INTRODUCTION

Nowadays, car air conditioning systems are state-of-the-art and standard equipment in most cars. They not only ensure the thermal comfort of the passengers, but in particular also improve driving safety, for example by keeping windows fog-free and ensuring a less tiring cabin environment. Over time, improvements have been made with regard to efficiency, robustness and environmental compatibility of the refrigeration cycle. The choice of suitable refrigerants went hand in hand with further developments. As a result of the Montreal Protocol, the initially widespread but ozone-depleting R12 was replaced by R134a, which, although it has an ODP value of 0, still has a high global warming potential with a GWP value of 1430. According to EU Directive 2006/40/EC, all refrigerants with a GWP of greater than 150 have been banned in new vehicles in the European Union since January 1st 2017. The newly developed R1234yf, which is used in many vehicles, has been established as an alternative to R134a. The advantage of R1234yf is a low GWP value of 4, as well as in the very similar fluid properties compared to R134a (Reasor *et al*., 2010), which is why an exchange of the refrigerants only involves little effort and no redevelopment of the various components is necessary. In addition to the flammability of R1234yf, one of the disadvantages compared to R134a is a slightly lower volumetric cooling capacity and system efficiency, which has been investigated by numerous authors (Navarro-Esbri *et al*., 2013; Wang, 2014; Zilio *et al*., 2011).
The replacement of the refrigerant is accompanied by an adaptation of the component modeling. The design and system simulation of the refrigeration cycle of the air conditioning system in the automobile is often done with the modeling language Modelica and the graphical interface Dymola. The individual components of the process are only resolved in one spatial dimension, whereby the connecting lines between the components are often completely neglected or modeled as straight pipes of the same length, although refrigerant lines are made up of a large number of bends, various extensions and constrictions, and flexible hose elements (see figure 1). This has the consequence that the resulting pressure drop is greatly underestimated in some cases, which leads to an overestimation of the calculated COP of the refrigeration cycle by up to 10% (Subei and Schmitz, 2018).
As a basis for this paper, an in-depth analysis of refrigerant pipes from a vehicle was conducted to examine the extend of pressure drops and their potential predictability using literature correlations or numeric flow simulations. The latter offer the advantage of a three-dimensional consideration of the complex geometry.

Figure 1: Automotive refrigerant pipe

2. TEST RIG

In order to experimentally determine the pressure drop of different line types, a test rig was planned and built at the Institute of Engineering Thermodynamics of the Hamburg University of Technology, with which the typical states in the respective line type can be set and measured. In addition, flow simulations using the Star-CCM+ software are carried out. The overall aim of the investigations is to improve 1D pipe models, which are required in detailed system simulations of the entire refrigeration cycle.

For the experimental investigations, the purpose of the test rig is to create a flow situation with a given state at the inlet of the test section. Oil-free R1234yf is used as refrigerant. Lubricating oil causes the pressure drop to raise, but is not the subject of this paper. For further investigations, refer to Chen et al. (2007). The operating conditions are based on those of a vehicle refrigeration system and range in temperature from -15 °C to 130 °C, in pressure from 2.5 bar to 30 bar and in mass flow up to 300 kg/h. Correspondingly overheated, subcooled or two-phase states can be set. In order to simplify the control of the system and the setting of two-phase states, the system works as a pump cycle. Figure 2 shows the system's process flow diagram.

The refrigerant enters a four-stage side channel pump on the suction side and is pumped to a higher pressure. Since a minimum flow rate is required, the mass flow is first measured on the pressure side and a partial mass flow is fed directly to the condenser via a bypass. The main mass flow is passed through a first sight glass so that it can be checked whether the fluid is in liquid state. This is necessary because the following mass flow sensor (measuring accuracy 0.1 % of the measured value) cannot measure correctly in two-phase states. The mass flow is regulated with a subsequent control valve, whereupon the refrigerant flows into a pre-evaporator. Like the condenser, it is designed as a plate heat exchanger and fed with hot thermal oil on the secondary side. The test section temperature is controlled directly via the thermal oil mass flow and the steam quality via an energy balance. After the pre-evaporator, the fluid flows through another sight glass into an inlet section with the flow being calmed down so that a developed velocity profile can establish. The inner diameter of the inlet section is always adapted to the inner diameter of the test section. This is followed by the variable test section over which the differential pressure is measured. In overheated states, the differential pressure lines to the sensor are heated so that no capillary forces due to condensing refrigerant influence the measurement. In subcooled states, the differential pressure lines are completely filled with liquid and are not heated. The main mass flow from the test section is then united with the partial mass flow from the bypass and subcooled in the condenser. The inlet pressure into the test section is set both via the system refrigerant charge and via the re-cooling temperature of the cold thermal oil in the condenser. The liquid refrigerant flows either through a tank or directly to the pump. For safety purposes, the system must not be completely filled with liquid. Therefore, if liquid lines are to be measured, the tank can be bypassed and heated so that the refrigerant is shifted from the tank to the test section. The heating and cooling peripherals are taken from a CO_2 system, which is described in more detail by Subei and Schmitz (2018). The measurement data acquisition and the system control is done with LabView. Piezoresistive sensors of the type Wika S20 or Wika DPT10 are used as sensors for pressure and differential pressure measurement. Pt100 sensors are used for temperature measurement. The measuring accuracy of the differential pressure measurement is ± 75 Pa, the accuracy of the temperature and pressure sensors is ± 0.08 K and ± 0.1 bar, respectively.

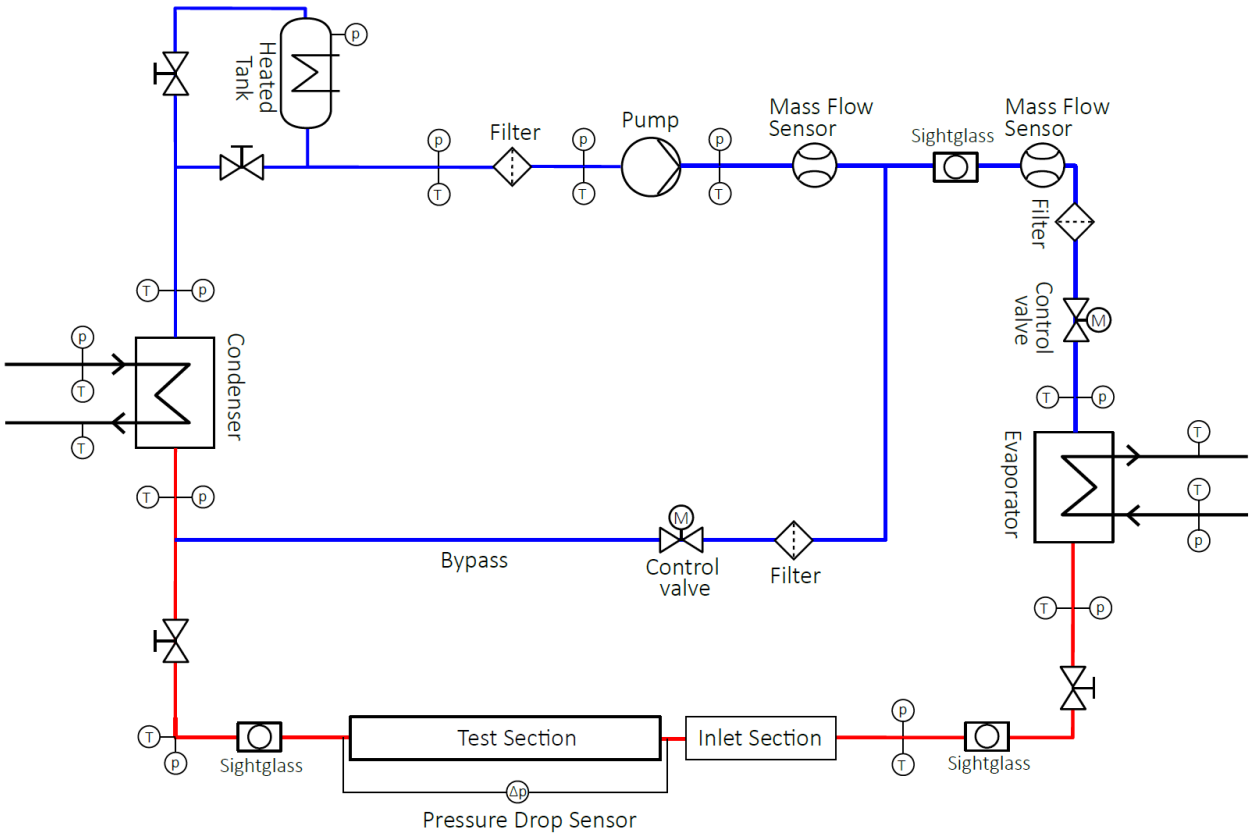

Figure 2: Process flow diagram of test rig

3. ANALYSIS OF A SINGLE HOSE ELEMENT

During the investigation of various pipes, it turned out that there is a large deviation between numerical results and the measured values. It is assumed that the reason lies in the numerous hose sections, as their internal structure is unknown. Therefore, in this section a single hose from a liquid line is examined as an example.
For the experiments, a liquid state is set at the inlet of the test section. The pressure is 13 bar and the temperature 45 °C, which corresponds to a subcooling of 5 K. The geometric dimensions of the hose can be found in Table 1. The differential pressure measurement already shows high values of up to 237 mbar at mass flows of 300 kg/h for the relatively short hose of 103 mm. Since the measured pressure drops are in the same order of magnitude as in much longer hoses, it can be assumed that the reason for this is not the surface roughness of the hose, but the transition pieces from aluminum pipe to hose.

Table 1: Dimensions of the single hose element

Type	Length *l* in mm	Inner Diameter *d* in mm
Pipe section inlet	40	7.5
Transition Piece	27	5
Hose	103	8
Transition Piece	27	5
Pipe section outlet	60	7.5

In order to check the CAD geometry, the hose is cut at the transition pieces along its main flow direction. The exposed transition piece can be seen in figure 3. The connection consists of a pipe end rolled onto the inside diameter of the

hose. In addition to the reduction in the outer diameter of the pipe, two grooves for O-rings are also rolled on for the sealing effect to the outside. After a look at the inside of the transition piece in figure 4, it is noticeable that these grooves can also be found inside the pipe in the form of two shoulders. This structure is not considered in the 3D CAD drawing. It is therefore subsequently added in the following and the influence on the pressure drop of the hose is numerically examined using CFD simulations.

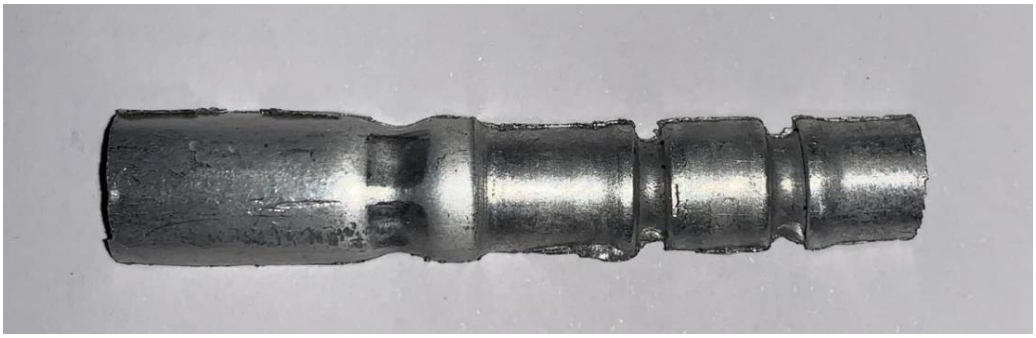

Figure 3: Liquid line transition piece outside

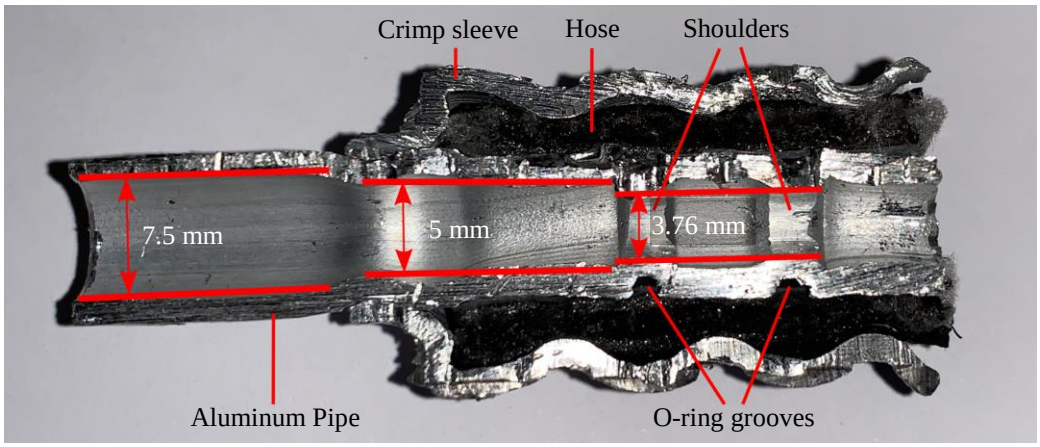

Figure 4: Liquid line transition piece inside

Since the shoulders inside the pipe are not exactly identical and are difficult to measure, they are approximated as a circular arc with a variable height, as shown in figure 5. Turbulence is represented in all the following 3D-CFD simulations using the RANS model. The eddy viscosity is modeled via the realizable kε two-layer model. The flow boundary layer near the wall is resolved in the transition piece and its wake using a low y+ grid and modeled in the tube and hose using a high y+ grid. All simulations are assumed to be stationary and in the case of liquid states constant fluid properties are used. Following a comprehensive grid independence study, the plausibility of the simulations is assessed. For this purpose, the velocity field at the hose transition is examined more closely in figure 6. It can be seen that the flow in the narrowest cross section of the pipe is accelerated from 4 m/s to double the velocity of 8 m/s and then decelerated again. It is also noticeable that the flow through the second shoulder is influenced by that of the first shoulder and that it takes a certain distance to calm the flow downstream. Dead zones are also visible in the corners of the hose.

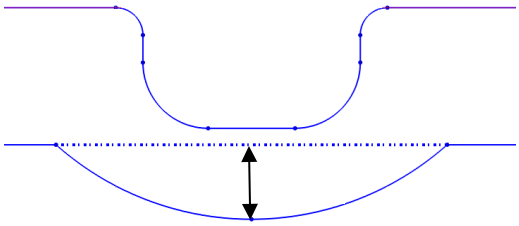

Figure 5: Outline of the shoulder model

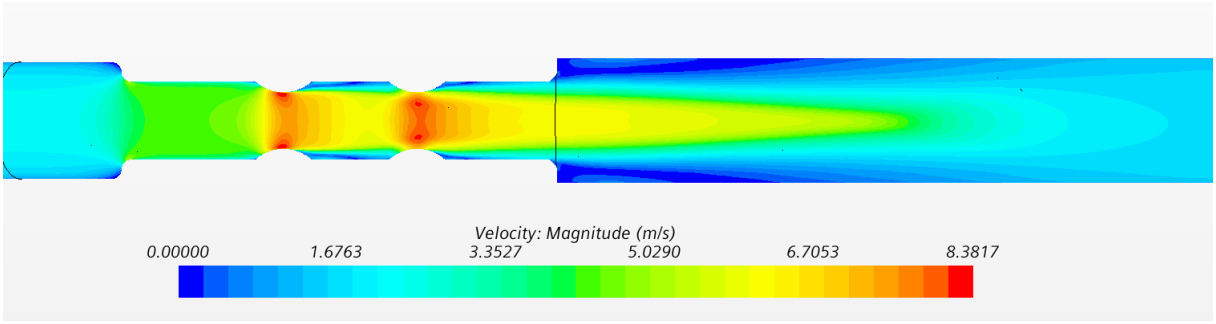

Figure 6: Velocity field in transition piece

In order to determine the influence of the shoulder height on the total pressure drop of the hose, this is varied in a parameter study. The results are shown in figure 7. It can be seen that there is an exponential relationship between shoulder height and pressure drop. If the pressure drop only changes a little at small heights, it increases from a height of 0.5 mm and the total pressure drop of the hose grows significantly. It should be mentioned that there is a total of four shoulders, each of which causes a throttling of the fluid. All simulations are carried out at 300 kg/h. It turns out that a shoulder height of 0.62 mm fits the experimental results best, whereas the simulation without a shoulder underestimates the measurement results by 44 %.

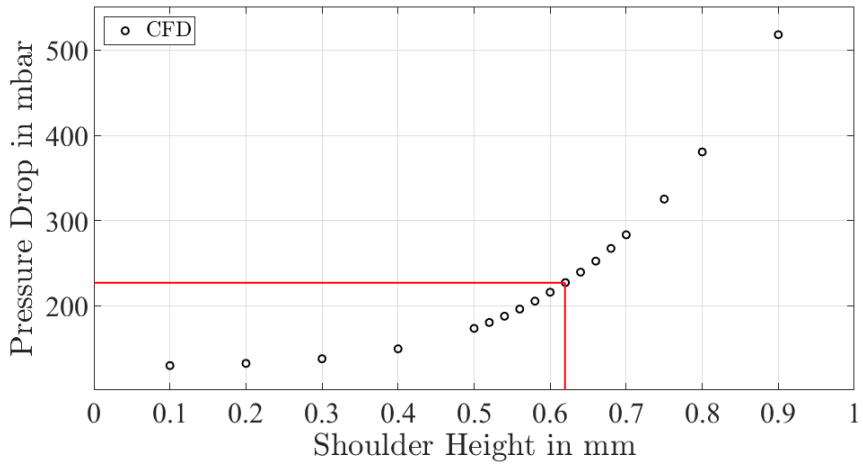

Figure 7: Influence of shoulder height on the hose pressure drop

4. ANALYSIS OF A LIQUID LINE

In the following, a liquid line from a vehicle is analyzed for its pressure drop. The line, shown in figure 1, is installed in the engine compartment of the vehicle and connects the condenser with the internal heat exchanger. The line consists of a large number of straight sections, bends and constrictions, as well as two hose elements. As with the single hose, the inlet pressure is 13 bar and the temperature 45 °C. Parallel to the experiments, both CFD flow simulations and

analytical calculations using the Colebrook-White correlation (Colebrook, 1939) are carried out. In this case, the entire line is assumed to be a straight pipe of the same length. Since this is a very strong simplification, a large deviation is expected. Nevertheless, this method is investigated for the sake of theory.
A comparison of the results is shown in figure 8, where the pressure drop is plotted against the mass flow. It turns out that the simplification of a straight pipe underestimates the experimental data by 88.8 % and is therefore the worst approach. The CFD simulation, which uses the original geometry without shoulders, delivers better results, but these are still 36.4 % below the experimental data. This shows that the shoulders have a major influence on the line, in particular because there are even two hose sections, i.e. a total of eight shoulders that act as a throttle. The shoulders in each transition piece are therefore added to the geometry also with a height of 0.62 mm. The results are also shown in figure 8. It can be seen that this measure greatly improves the simulation results, even though the hose investigated in the previous section comes from a different liquid line. In this case, the deviations from the measurement results are only -1.0 %, which is why the improved CFD simulation is now suitable for predicting pressure drops. Furthermore, these results confirm the shoulders as the reason for the previous deviation and thus as a geometric detail that should not be neglected. Simulations can now be carried out for all lines with the same inner dimensions with a good prediction accuracy.

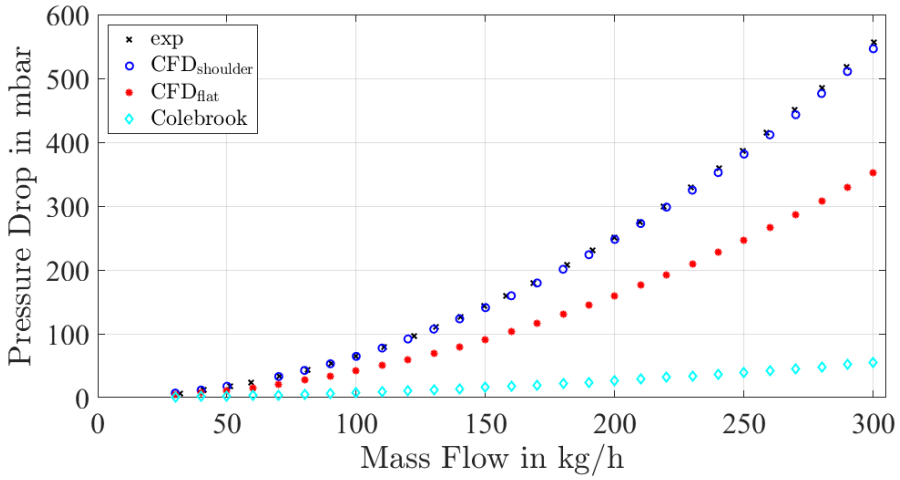

Figure 8: Pressure drop curve of the liquid line for different approaches

Finally, the results are de-dimensioned and plotted as a drag coefficient over the Reynolds number in figure 9. A fit of this curve can now be used in a model of the line for the system simulation so that other liquid states can also be represented.

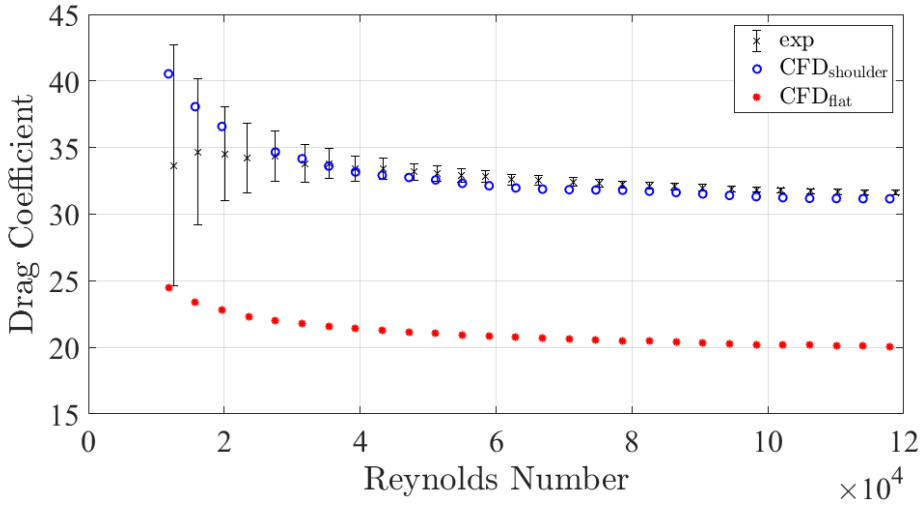

Figure 9: Drag coefficient curve of the liquid line in dependency of the Reynolds number

5. ANALYSIS OF A HOT GAS LINE

In the previous section only liquid states are investigated. In that case the dependence of the density from the pressure is negligible, which is why an incompressible model is used. In hot gas lines, however, as the name says, flows are in gaseous state. The question therefore arises whether the simplification of an incompressible fluid is still justified. Since it is expected that the density will change significantly, the influence of the compressibility of the gas is investigated in this section for different pressures. For this purpose, the density field with the dependence on pressure and temperature is implemented as a two-dimensional polynomial in the model keeping all other properties constant. The fluid properties are taken from Refprop (Richter *et al.*, 2011). In the case of compressible flows, a dropping pressure leads to a reduction in density. Since there is a constant mass flow, the refrigerant should be accelerated according to the continuity equation for a constant cross section. Since the pressure drop is proportional to the square of the velocity, it should increase significantly compared to an incompressible flow.
For the hot gas line, it has to be clarified whether the line also has shoulders at the transition piece right as the slightly smaller liquid line. Since the hose connection looks identical from the outside to that of the liquid line and since two grooves for O-rings can also be recognized in the CAD file, shoulders with the same height of 0.62 mm are subsequently added to this geometry. The investigated hot gas line is shown in figure 10.

Figure 10: Hot gas line

The measurement values are compared to the results of the CFD simulation in figure 11. The pressure at the inlet is 8 bar and the temperature 45 °C. It is first noticeable that very large pressure drops of up to 2.3 bar at 260 kg/h were measured. In this case the density changes by -30 % so that the assumption of incompressibility is no longer justified. However, it also shows that the measured values correspond more closely to the results of the incompressible simulation and that the compressible model greatly overestimates the pressure drop and becomes unstable from 180 kg/h on. It should also be pointed out that the measured values no longer correspond to the typical quadratic curve of the incompressible curve.

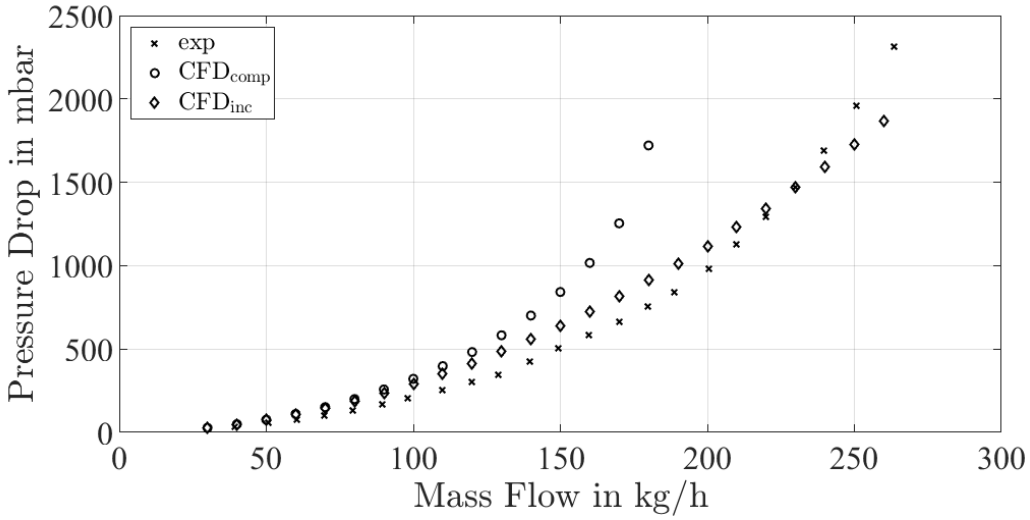

Figure 11: Pressure drop curve of hot gas line with internal shoulders being considered

In order to find the reason for these deviations, the hot gas line is also cut along its main flow direction and investigated. The transition piece can be seen in figure 12. It turns out that in this case there is an extension of the pipe's inner diameter at the position of the O-ring grooves, so that the shoulders no longer protrude into the main flow. Therefore, the manually added shoulders are removed again so that the geometry only contains the constriction caused by the rolled pipe end and the simulation is carried out again. The results can be seen in figure 13. The three states at the inlet correspond to 8 bar and 45 °C, 14 bar and 70 °C, as well as 20 bar and 90 °C.

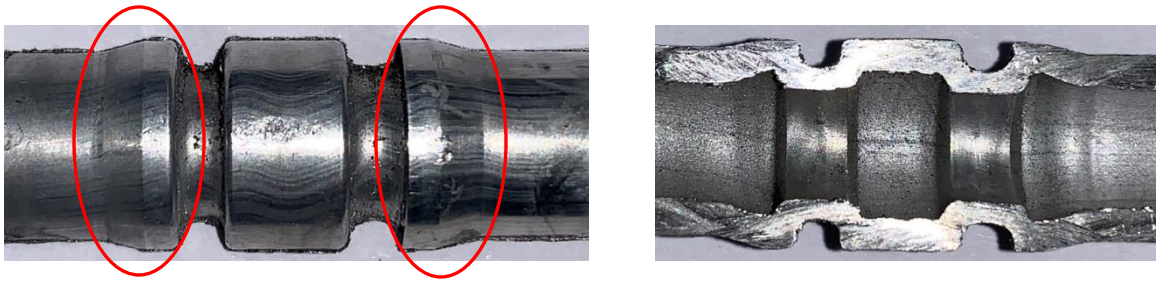

a) b)

Figure 12: Hot gas line transition piece

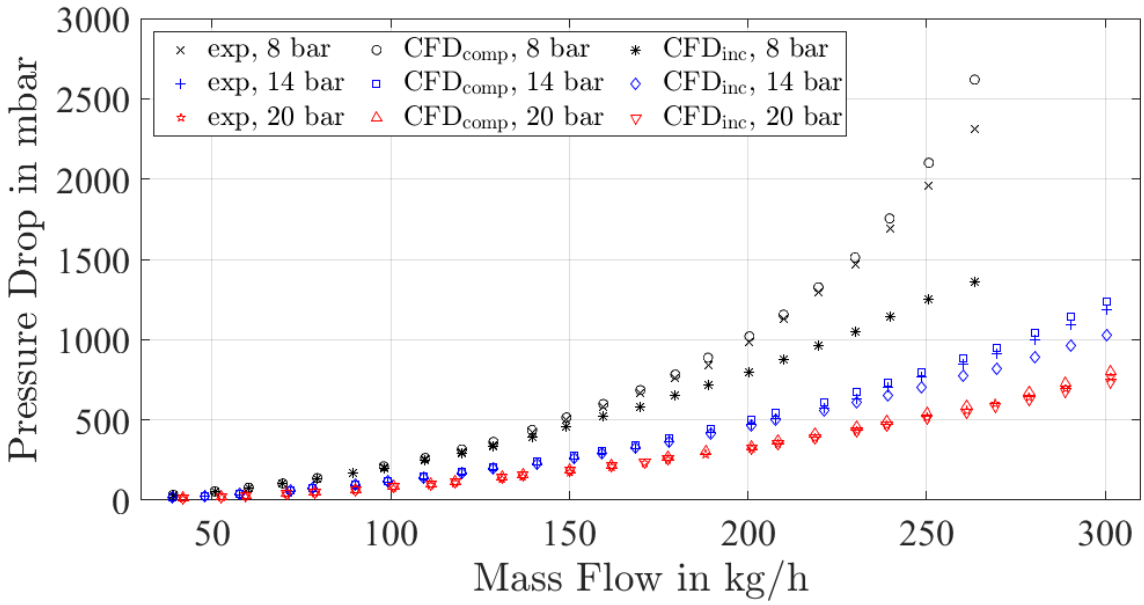

Figure 13: Pressure drop curve of hot gas line without internal shoulders being considered

It can be seen that the compressibility of the gas has a greater influence on the pressure drop at low pressures. This is demonstrated at the state of 8 bar. With large mass flows, the pressure drop no longer increases quadratically, but more steeply. The compressible CFD model is able to reproduce the measured values well even with mass flows of above 150 kg/h. With a mass flow of 260 kg/h, the pressure between the inlet and outlet decreases by -31.9 % and the density by down to -36.3%. It should be mentioned that the acceleration of the gas in the transition piece causes the static pressure to drop, resulting in a local density even below the value at the outlet. With increasing pressures, the influence of compressibility decreases significantly, whereby the compressible results are again closer to those of the incompressible model. Table 2 shows the mean errors of the simulations compared to the experiments, as well as the decrease in pressure and density occurring at each maximum mass flow. The conclusion for this section is that it very much depends on which state is to be investigated. If only higher pressures are to be analyzed an incompressible model can cover the physics sufficiently.

Table 2: Relative pressure drop, density drop and errors

Simulation	Δp_{max} in %	$\Delta \rho_{max}$ in %	MRD in %	MARD in %
CFD 8 bar incompressible	-16.6	0	-12.6	12.6
CFD 8 bar compressible	-31.9	-36.3	3.5	3.9
CFD 14 bar incompressible	-7.2	0	0.5	7.0
CFD 14 bar compressible	-8.7	-11.5	7.2	7.7
CFD 20 bar incompressible	-3.7	0	6.9	8.1
CFD 20 bar compressible	-4.0	-5.8	10.7	10.7

6. CONCLUSION

In this paper the pressure drop of vehicle refrigerant pipes is investigated. The aim is to improve 1D models for simulating the entire refrigeration cycle in the vehicle. For this purpose, an R1234yf test system was set up, with which all line types can be measured at the appropriate states. Using the example of a liquid and a hot gas line, the pressure drops over the entire lines are measured for different mass flows and it is investigated to what extent these can be predicted with numerical field simulations. To check the influence of hose components, a single hose is first measured and numerically investigated with a CFD simulation. This results in larger deviations from simulation and experiment. In order to check whether the CAD geometry contains all the relevant details after production, the hose is cut open along the main flow direction. There are two grooves for O-rings, which can be found in the CAD drawing on the outside of the pipe, but not inside. After taking these additional shoulders into account and adjusting the height, the CFD simulations for the single hose agree well with the measurement data. It turns out that the prediction accuracy of the liquid line could also be greatly improved with the implementation of these details.

In case of the hot gas line, it turns out that although the same connection technology is used for the hose transitions, there is a different internal structure. Therefore, the shoulders on the inside of the pipe no longer influence the pressure drop and can be neglected. It also shows that the inlet state has a major influence on whether the compressibility of the gas has to be considered. This is the case with low pressures and large mass flows, since the density changes by up to 36.3 % here. For higher pressures, the use of an incompressible model is justified. With the knowledge gained, it is possible to reduce the pressure drop of the lines, for example by adding an extension at the position of the shoulders to the liquid lines or by rolling the grooves for the O-rings less deep.

In further works it will be investigated to what extent the production of the pipes affects the variability of the internal structure at the hose transition. For this purpose, the inside of all transition pieces will be captured with a stylus device. Furthermore, it will be investigated how much the internal volume can be reduced if a constant pressure drop is taken as a basis, but with an optimized transition structure. Finally, a system simulation of the entire refrigeration cycle should be conducted to clarify how the pressure drop of the lines affect the system efficiency.

NOMENCLATURE

d	diameter	(m)
l	length	(m)
$\dot{m}$	mass flow	(kg/h)
p	pressure	(bar)
Δp	pressure drop	(bar)
ρ	density	(kg/m³)
Re	Reynolds number	(-)
T	temperature	(°C, K)
w	velocity	(m/s)
ζ	drag coefficient	(-)
z	height	(m)

Subscripts

CAD	computer aided design
CFD	computational fluid dynamics
comp	compressible
COP	coefficient of performance
exp	experimental
flat	flat
GWP	global warming potential
inc	incompressible
MARD	mean absolute relative deviation
max	maximum
MRD	mean relative deviation
ODP	ozone depletion potential
shoulder	with shoulders

REFERENCES

Chen, I. Y. *et al.* (2007). Two-phase frictional pressure drop of R-134a and R-410A refrigerant-oil mixtures in straight tubes and U-type wavy tubes. *Experimental Thermal and Fluid Science, 31 (4)*, 291-299.

Colebrook, C. F. (1939). Turbulent flow in pipes with particular reference to the transition region between the smooth and rough pipe laws. *Journal of the Institution of Civil Engineers., 11* (4), 133-156.

Navarro-Esbrí, J. *et al.* (2013). Experimental analysis of R1234yf as a drop-in replacement for R134a in a vapor compression system. *International Journal of Refrigeration, 36*, 870-880.

Reasor, P., Aute, V. & Radermacher, R. (2010). Refrigerant R1234yf Performance Comparison Investigation. *International Refrigeration and Air Conditioning Conference*, Purdue University, Paper 1085.

Richter, M., McLinden, M.O. & Lemmon, E.W. (2011). Thermodynamic Properties of 2,3,3,3-Tetrafluoroprop-1-ene (R1234yf): Vapor Pressure and p-rho-T Measurements and an Equation of State. *Journal of Chemical & Engineering Data, 56* (7), 3254-3264.

Subei, C., Schmitz, G. (2018). Investigation of the Pressure Drop in Refrigerant Pipes of an R744 Automotive Air Conditioning System. *International Refrigeration and Air Conditioning Conference*. Purdue University, Paper 1938.

Wang, C.C. (2014). System performance of R-1234yf refrigerant in air-conditioning and heat pump system - An overview of current status. *Applied Thermal Engineering*, *73*, 1412-1420.

Zilio, C. *et al.* (2011). The refrigerant R1234yf in air conditioning systems. *Energy, 36*, 6110-6120.